Manuscript prepared for Nat. Hazards Earth Syst. Sci. Discuss.
with version 2014/09/16 7.15 Copernicus papers of the LaTeX class copernicus.cls.
Date: 26 December 2014

Brief Communication: Contrast stretching and histogram smoothness based flood detection

F. Nazir, M. M. Riaz, A. Ghafoor, and F. Arif

College of Signals, National University of Sciences and Technology (NUST),
Islamabad, Pakistan

Correspondence to: A. Ghafoor (abdulghafoor-mcs@nust.edu.pk)

Abstract

Synthetic aperture radar images used for flood detection often have degraded contrast, which consequently leads to inaccurate flood maps. A three steps approach (based on adaptive histogram clipping, histogram remapping and smoothing) is proposed for generation of a more visualized flood map image. The proposed scheme passes the pre and post flood images from adaptive histogram equalization while the difference image is passed through contrast enhancement and constraint based histogram smoothing for enhancement of hidden details. A fast ready flood map is then generated using equalized pre, post and difference images. Results are evaluated using different data sets which show significance of the proposed technique.

1 Introduction

Flood detection/mapping is desirable in variety of applications like disaster management, risk/damage assessment and rehabilitation process. Flood mapping/monitoring techniques use pre and post Synthetic Aperture Radar (SAR) images to classify non flooded and flooded (inundated) areas (Kussel et al., 2011; Nazir et al., 2013). However, SAR images often contain speckle noise which results in unwanted artifacts and contrast degradation. Different pre-processing techniques like (spatial and transform based) filtering are applied (before flood detection) to overcome these issues.

Visual interpretation (Chambenoit et al., 2003) requires user's involvement for the identification of flooded areas (which is not always feasible). Semi automatic segmentation based flood detection techniques generally require empirical seed point selection (Dellepiane et al., 2010; Martinis et al., 2011). Thresholding based unsupervised flood classification (Moser and Serpico, 2006) does not work under complex environmental conditions (in that case users involvement is required for reliable results) (Pulvirenti et al., 2011). Texture matching based scheme (Zhao et al., 2011) suffers from high computational time and overlapping features.

Schumann et al. (2009) have applied different processing steps to generate inundation maps, however it suffers from reliable calibration and verification. Complex coherence maps are used for the analysis of SAR data for flood monitoring, however, optical images are required for result verification (Chini et al., 2012). Dellepiane and Angiati (2012) flood monitoring technique sometimes highlight unnecessary details in the flood map. Matgen et al. (2011) proposed a hybrid flood extraction technique by combining region growing and radiometric thresholding. Giustarini et al. (2013) proposed an automated flood extent extraction scheme using backscatter thresholding, region growing and change detection techniques.

A three steps approach (based on Adaptive Histogram Clipping (AHC), Histogram Remapping (HR) and Histogram Smoothness (HS)) is proposed for generation of a more visualized RGB flood map image. The proposed technique follows the basic methodology proposed by (Dellepiane and Angiati, 2012) with certain modifications/improvements. More specifically the proposed scheme passes the pre and post flood images from adaptive histogram equalization while the difference image is passed through contrast enhancement and constraint based HS for enhancement of hidden details. A fast ready flood map is then generated using equalized pre, post and difference images. Results are evaluated using different data sets which show significance of the proposed technique.

2 Proposed methodology

Let $I_{X(l,m)}$ be pre, $I_{Y(l,m)}$ be post and $I_{Z(l,m)}$ be the difference image, where $l \in [0,\ldots,L-1]$ and $m \in [0,\ldots,M-1]$. Figure 1 shows the block diagram of proposed technique.

The histogram of pre image I_X is clipped (identical to (Dellepiane and Angiati, 2012), but with a low percentile value i.e. $q = 0.40$) to obtain I_{X1}. Note that low percentile values can remove desired details whereas high percentile values can highlight unwanted details. Therefore, an optimal value if percentile value should be used to preserve the intensity values (which contribute to flooding). After AHC, the image I_{X1} is remapped to original intensity range [0–255] using simple linear scaling (Dellepiane and Angiati, 2012) to obtain I_{X2}.

In next step, HS is applied to improve the visualization by preserving the details. In contrast to Dellepiane and Angiati (2012), which uses simple Histogram Equalization (HE), we have used HS to maintain the natural look, suppressing unwanted artifacts and enhancing the desired details.

In HS, a smoothness constraint is added to remove abrupt changes using backward difference K (Arici and Dikbas, 2009). The principle is to minimize the difference between modified h_{X2_m} and current h_2 histograms such that the modified histogram is also closer to the uniform histogram h_{X2_u} with an additional penalty term $\beta\|Kh_2\|$ (added for smoothness) i.e.,

$$\min \|h_{X2_m} - h_2\|_2^2 + \alpha\|h_{X2_m} - h_{X2_u}\|_2^2 + \beta\|Kh_2\|_2^2. \quad (1)$$

The solution to above constraint problem is (Arici and Dikbas, 2009),

$$h_{X2_m} = ((1+\alpha)\mathbf{I} + \beta(K)^T K)^{-1} \times (h_2 + \alpha h_{X2_u}), \quad (2)$$

where, $\mathbf{I}$ is identity matrix, α, β are the contrast enhancement and smoothness parameters (chosen empirically as 0.5 and 1000 respectively). The histogram h_{X2_m} is then used as a mapping function for HE to generate image I_{X3}. All three steps (AHC, HR and HS) are applied on I_Y (post flooded image) to generate I_{Y3}.

The difference image I_Z is generated as,

$$I_Z(l,m) = 128 + \frac{I_{X3}(l,m) - I_{Y3}(l,m)}{2}. \quad (3)$$

The pre and post flood images I_X and I_Y are passed through CE step to produce $\hat{I}_X$ and $\hat{I}_Y$ respectively. The reason for skipping the first two steps is to preserve intensity values of pre and post images. The processed pre and post flooded images for difference image generation is to remove the intensities which contribute very low in flooded areas. Finally $I_Z, \hat{I}_X$ and $\hat{I}_Y$ are combined (by assigning red, blue and green bands) to generate fast ready map. The level of red color is high for pixels whose pre value dominates and vice versa. Red (medium to dark) color represents the permanent water (like rivers) while the dark blue color represents flooded areas.

3 Simulation and results

Existing and proposed techniques are evaluated on different SAR images. Figure 2a and b shows pre and post flood images of ChoeleChoele City, Argentina observed by “Daichi” (ALOS) on 29 April and 30 July 2006 respectively. Figure 2c and d show the difference images obtained using Dellepiane and Angiati (2012) and proposed technique respectively. In Fig. 2c, the ground details are more prominent while Fig. 2d only highlights the major required details comparatively. The differences in detail contribute significantly to their respective RGB image (shown in Fig. 2e and f). In Fig. 2e, a very high contribution of irrelevant details (of difference image) is visible (for instance, the blue color at the center and at the top right corner). Figure 2f provides better visibility of flooded areas around river (at the top center) and low flooded areas (at the center (below river) and top right corner) of the image.

Figure 3a and b show the images of Tomakomai, Japan, acquired by Phased Array Type L-band SAR (PALSAR) using H/V and V/V polarization on 19 August 2006 respectively. Figure 3c is the RGB flood map generated using Dellepiane and Angiati (2012) technique. The flood map (in Fig. 3c) highlights some irrelevant details which contribute to flooding (blue colored areas at the right center of the image). Figure 3d shows the flood map generated using the proposed technique. Figure 3d preserves the natural effect of image as compared to Fig. 3c.

4 Conclusions

A technique for flood detection based on contrast stretching and histogram smoothing is presented. Different processing steps based on contrast stretching and histogram smoothness are applied on pre, post and difference images to generate flood maps. Simulation results show improved visualization by maintaining the natural smoothness.

References

Arici, T. and Dikbas, S.: A histogram modification framework and its application for image contrast enhancement, IEEE T. Image Process., 18, 1921–1935, 2009.

Chambenoit, N., Classeau, E. T., and Rudant, J. P.: Performance assessment of multitemporal SAR images' visual interpretation, IEEE International Geoscience and Remote Sensing Symposium, Toulouse, France, 21–25 July 2003, vol. 6, 3911–3913, doi:10.1109/IGARSS.2003.1295311, 2003.

Chini, M., Pulvirenti, L., and Pierdicca, N.: Analysis and interpretation of the Cosmo-SkyMed observations of the 2011 Japan Tsunami, IEEE Geosci. Remote S., 9, 467–471, 2012.

Dellepiane, S. and Angiati, E.: A new method for cross-normalization and multitemporal visualization of SAR images for the detection of flooded areas, IEEE T. Geosci. Remote, 50, 2765–2779, 2012.

Matgen, P., Hostache, R., Schumann, G., Pfister, L., Hoffmann, L., and Savenije. H.H.G.: Towards an automated SAR-based flood monitoring system: Lessons learned from two case studies, Physics and Chemistry of the Earth, 36, 241–252, 2011.

Giustarini, L., Hostache, R., Schumann, G.J.-P., Matgen, P., Bates, P.D., and Mason. D.C.: A change detection approach to flood mapping in urban areas using TerraSAR-X, IEEE T. Geosci. Remote, 51, 2417–2430, 2013.

Dellepiane, S., Angiati, E., and Vernazza, G.: Processing and segmentation of cosmo-skymed images for flood monitoring, IEEE International Geoscience and Remote Sensing Symposium, 4807–4810, 2010.

Martinis, S.; Twele, A.; Voigt, S.: Unsupervised extraction of flood-induced backscatter changes in SAR data using Markov image modeling on irregular graphs, IEEE T. Geosci. Remote , 49, 251–263, 2011.

Kussul, N., Shelestov, A., and Skakun, S.: Flood monitoring from SAR data, NATO Science for peace and security series C, Environmental Security, 9–29, 2011.

Moser, G. and Serpico, S. B.: Generalized minimum-error thresholding for unsupervised change detection from SAR amplitude imagery, IEEE T. Geosci. Remote, 44, 2972–2982, 2006.

Nazir, F., Riaz, M. M., Ghafoor, A., and Arif, F.: Contrast enhancement based flood monitoring, IEEE International Symposium on Intelligent Signal Processing and Communication Systems, Okinawa, Japan, 12–15 November, 2013.

Pulvirenti, L., Pierdicca, N., Chini, M., and Guerriero, L.: An algorithm for operational flood mapping from Synthetic Aperture Radar (SAR) data using fuzzy logic, Nat. Hazards Earth Syst. Sci., 11, 529–540, doi:10.5194/nhess-11-529-2011, 2011.

Schumann, G., Baldassarre, G. D., and Bates, P.: The utility of spaceborne radar to render flood inundation maps based on multialgorithm ensembles, IEEE T. Geosci. Remote, 47, 2801–2807, 2009.

Wang, Q. and Ward, R. K.: Fast image/video contrast enhancement based on weighted thresholded histogram equalization, IEEE T. Consumer Electr., 53, 757–764, 2007.

Zhao, M., Shang, H., Huang, W., Zou, L., and Zhang, Y.: Flood area extraction from rgb aerophotograph based on chromatic and textural analysis, International Conference on Advanced Geographic Information Systems, Appliations and Services GeoProcessing, 46–52, 2011.

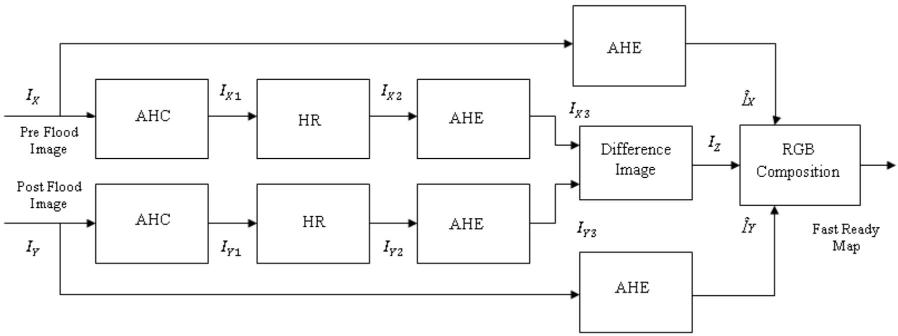

Figure 1. Flow chart of proposed algorithm.

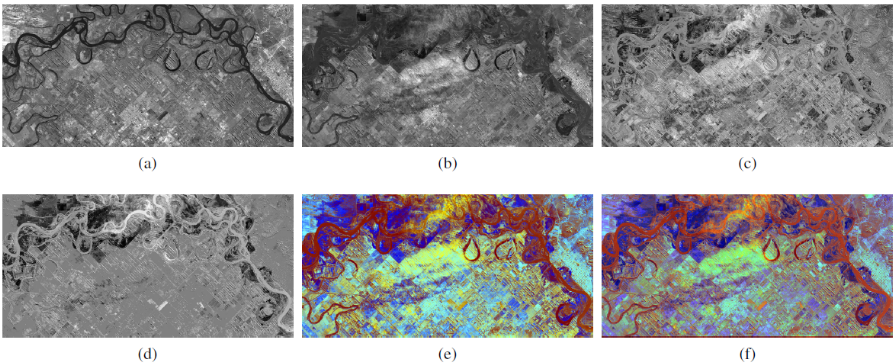

Figure 2. Original images of ChoeleChoele City, Argentina observed by “Daichi” (ALOS): **(a)** pre flooded image acquired on 29 April 2006. **(b)** Post flooded image acquired on 30 July 2006. **(c)** Difference image obtained using Dellepiane and Angiati (2012) technique. **(d)** Difference image obtained using proposed technique. **(e)** Fast ready map generated using Dellepiane and Angiati (2012) technique. **(f)** Fast ready map generated using proposed technique.

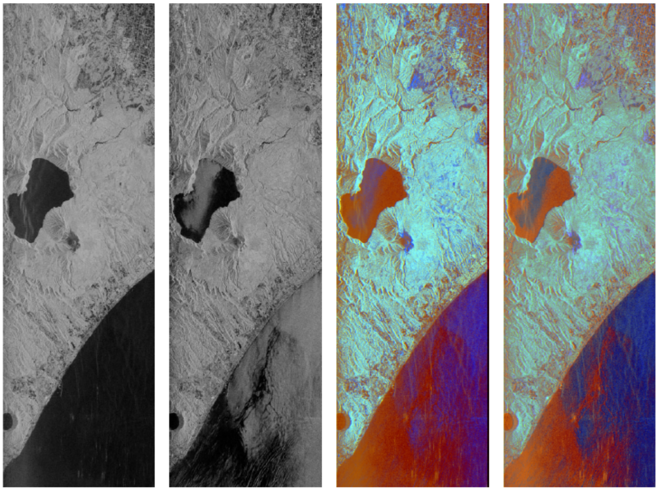

Figure 3. Evaluation of results using images of Tomakomai, Japan. **(a)** Pre image acquired on 19 August 2006. **(b)** Post image acquired on 19 August 2006. **(c)** Fast ready map generated using Dellepiane and Angiati (2012) technique. **(d)** Fast ready map generated using proposed technique.